Atmos. Chem. Phys. Discuss., https://doi.org/10.5194/acp-2017-649
Manuscript under review for journal Atmos. Chem. Phys.
Discussion started: 4 August 2017

Atmospheric Chemistry and Physics Discussions

The aerosol-cyclone indirect effect in observations and high-resolution simulations

Daniel T. McCoy[1], Paul R. Field[1,2], Anja Schmidt[1], Daniel P. Grosvenor[1], Frida A.-M. Bender[3], Ben J. Shipway[2], Adrian A. Hill[2], Jonathan M. Wilkinson[2]

[1]University of Leeds, Leeds LS2 9JT, UK
[2]Met Office, Fitzroy Rd, Exeter EX1 3PB, UK
[3]University of Stockholm, Svante Arrhenius Väg 16C, Sweden

Correspondence to: Daniel T. McCoy (D.T.McCoy@leeds.ac.uk)

Abstract. Aerosol-cloud interactions are a major source of uncertainty in predicting 21st century climate change. Using high-resolution, convection-permitting global simulations we predict that increased cloud condensation nuclei (CCN) interacting with midlatitude cyclones will increase their cloud droplet number concentration (CDNC), liquid water (CLWP), and albedo. For the first time this effect is shown with 13 years of satellite observations. Causality between enhanced CCN and enhanced cyclone liquid content is supported by the 2014 eruption of Holuhraun. The change in midlatitude cyclone albedo due to enhanced CCN in a surrogate climate model is around 70% of the change in a high-resolution convection-permitting model, indicating that climate models may underestimate this indirect effect.

1. Introduction

The degree to which the aerosol indirect effects that result from anthropogenic aerosol emissions have acted to increase planetary albedo and mask greenhouse gas warming is highly uncertain (Andreae et al., 2005;Carslaw et al., 2013;Boucher et al., 2014;Forster, 2016). Establishing how much aerosol emitted during the 20th century has enhanced the liquid water amount and thus the albedo of midlatitude storm systems is a key step in constraining predictions of 21st century warming. Extratropical cyclones play an important role in the transport of moisture, heat, and momentum as well as in determining midlatitude albedo (Hartmann, 2015). They are formed by thermal contrast between the subtropics and polar regions. However, based on observational case-studies and modelling it is known that both the synoptic-scale atmospheric processes and much smaller scale cloud microphysical processes play a role in regulating the cyclone lifecycle (Naud et al., 2016;Grandey et al., 2013;Lu and Deng, 2016;Thompson and Eidhammer, 2014;Igel et al., 2013).

In general for warm rain processes, enhanced aerosol that can act as cloud condensation nuclei (CCN) should enhance cloud droplet number concentration (CDNC, the first indirect, or Twomey effect) (McCoy et al., 2017;Nakajima et al., 2001;Charlson et al., 1992;Twomey, 1977). This effect has the potential to suppress precipitation and lead to a greater retention of liquid water within the cloud (the second indirect, lifetime, or Albrecht effect) (Albrecht, 1989;Gryspeerdt et al., 2016;Sekiguchi et al., 2003). Empirical studies have established some evidence supporting the existence of these effects in liquid clouds (Gryspeerdt et al., 2016;Quaas et al., 2008;Nakajima et al., 2001;Sekiguchi et al., 2003;McCoy et al., 2017;McCoy et al., 2015;Meskhidze and Nenes, 2006), although it has been argued that compensating physical processes

may offset these microphysical perturbations(Stevens and Feingold, 2009;Malavelle et al., 2017). However, aerosol-cloud indirect effects have not been previously observed on a global scale in extratropical cyclones. Here we use global high-resolution simulations and remote-sensing observations to show that aerosol-cloud interactions produce an increase in the cloud liquid water content and albedo of extratropical cyclones. Further observational evidence is supplied by the natural laboratory provided by a degassing volcano in the North Atlantic. Some recent studies have used volcanoes to show that transient changes in aerosol load lead to changes in cloud properties (Mace and Abernathy, 2016;Gassó, 2008;Ebmeier et al., 2014;Yuan et al., 2011;McCoy and Hartmann, 2015;Schmidt et al., 2012;Malavelle et al., 2017), but due to the difficulty in separating meteorological and aerosol effects this is the first time that a liquid water response has been demonstrated for extratropical cyclones.

In the next section we will discuss the synthesis of observations, idealized simulations of cloud responses to aerosol, and volcanic plume modelling used to disentangle the effects of aerosols and meteorology on clouds. In section 3 we present our analysis of our idealized aquaplanet simulations, we test the hypothesis arrived at in these simulations in the observational record, and using the 2014-2015 Holuhraun eruption. In section 4 we summarize our results and consider how they relate to predicting 21st century climate change.

2. Methods

2.1 Observations

The Modern-Era Retrospective Analysis for Research and Applications version 2(Bosilovich et al., 2015) (MERRA2) sea level pressure (SLP) was used to composite observations from the Advanced Microwave Scanning Radiometer(Wentz and Meissner, 2000) (AMSR2 and AMSRE) and reanalysis data from MERRA2 around cyclone centers during the period 2003-2015. Cyclone compositing was performed following the algorithm in Field and Wood (2007). Supporting observations of CDNC from Moderate Resolution Imaging Spectroradiometer (MODIS) (King et al., 2003) were also composited on MERRA2 SLP and were filtered as dictated by previous studies to reduce biases associated with inhomogeneous clouds and low sun angle and cloud tops were restricted to be below 3.2km (Grosvenor and Wood, 2014). CDNC from MERRA2 was calculated following the regression model relating log sulfate mass concentration to log CDNC presented in previous studies (McCoy et al., 2017). Data from the CERES SYN1DEG data set edition 3(Wielicki et al., 1996) were used to examine cyclone albedo and cloud fraction. Mean solar insolation between 30°-80° was calculated using the CERES EBAF-TOA edition 4 data set(Loeb et al., 2009).

Because microwave radiometers must make assumptions regarding the partitioning of precipitating and non-precipitating liquid we calculated the rain water path following the parameterization used to retrieve AMSR rain rate(Wentz and Meissner, 2000) using the AMSR-observed sea surface temperature (SST) combined with the Marshall-Palmer size distribution (Marshall and Palmer, 1948), and the terminal fall speed relations presented in Hill et al. (2015).

Atmos. Chem. Phys. Discuss., https://doi.org/10.5194/acp-2017-649
Manuscript under review for journal Atmos. Chem. Phys.
Discussion started: 4 August 2017

2.2 Simulations

2.2.1 Aquaplanet

Two sets of simulations in the MetOffice Unified Model (UM) vn10.3 based on GA6 (Walters et al., 2017) were created to test the sensitivity of the cloud-aerosol indirect effect to model resolution in an idealized aquaplanet setting. These models were a typical, GCM-surrogate model and a convection-permitting model. The GCM-surrogate model was run at 1.89°x1.25° and incorporated a parameterized convection scheme. The convection-permitting model was run at 0.088°x0.059° and no convection parametrization was used. Both simulations were run with 70 vertical levels. The Cloud-AeroSol Interacting Microphysics (CASIM) two-moment microphysics scheme (Hill et al., 2015;Shipway and Hill, 2012;Grosvenor et al., 2017) was used for all clouds in the convection-permitting simulation and for large-scale cloud cover in the GCM-surrogate simulation. Sea surface temperature (SST) was held fixed in the simulations and the atmosphere was allowed to spin up for a week at low resolution and then for another week at high resolution. The SST profile used in the aquaplanet was derived from a 20-year climatology run from the UM in standard climate model configuration. The January SST was averaged with a north-south reflected version of itself and then zonally averaged to provide a symmetrical SST. The aerosol profile in the control simulation was 100/cc in the accumulation mode at the surface and then exponentially decreasing after 5km with an e-folding of 1 km. Aerosol cloud interactions were parameterized using a simple Twomey-type parameterization(Rogers and Yau, 1989) with $CDNC = 0.5Nw^{0.25}$ with N being accumulation mode aerosol number concentration and w being updraft velocity limited such that at w=16m/s CDNC=N, and w has a minimum value of 0.1m/s. Aerosol was non-interacting. The effects of enhanced aerosol on clouds was investigated by increasing aerosol at the surface to 2000/cc in a channel between 30°N and 60°N. Ice number was controlled using a simple temperature-dependent relationship (Cooper, 1986). Simulations were then run for 15 days.

2.2.2 Holuhraun eruption

To evaluate which cyclones had interacted strongly with the sulfur emitted by Holuhraun simulations were run with nudged meteorology in the Lagrangian dispersion model, NAME (Schmidt et al., 2015;Jones et al., 2007). The simulations were set-up using a time varying flux of SO_2 of 100 kt/d between 31 August 2014 and 13 September 2014 and 60 kt/d thereafter in line with observations and fluxes derived in a previous study (Schmidt et al., 2015). Emissions were distributed uniformly between 1500-3000m, consistent with the emission height during September(Schmidt et al., 2015). Sensitivity to emission height was tested using a second simulation with emissions between 0-1500m. The near-surface sulfate was calculated by taking the mean over the bottom five model levels (100m-900m).

Atmos. Chem. Phys. Discuss., https://doi.org/10.5194/acp-2017-649
Manuscript under review for journal Atmos. Chem. Phys.
Discussion started: 4 August 2017

Atmospheric Chemistry and Physics Discussions

3. Results and discussion

3.1 Observed relations between meteorology, cyclones, and aerosol

Compared to the meteorological drivers of cyclone formation, aerosol-cloud interactions are subtle and difficult to observe. However, by using model simulations we can add or remove aerosol to disentangle aerosol-induced alterations to midlatitude storms from the meteorology driving them. We created a suite of simulations in the MetOffice Unified Model (UM) that explores aerosol-cloud interactions. Because the focus of this study is to understand maritime, midlatitude storms the model has no land surface (an aquaplanet) allowing an unbroken storm track providing more cyclones to be analyzed without the complications of landmasses on their evolution. The model resolution was high enough (6.5km in the midlatitudes) to permit convection to be resolved by the model. To understand the behavior of a typical GCM participating in the climate model intercomparison project (CMIP) a second set of simulations at a GCM-surrogate resolution (140km in the midlatitudes) was created. In the convection-permitting model no convection parameterization was used, meaning that all clouds were treated by the same cloud microphysics(Shipway and Hill, 2012). In the GCM-surrogate model the UM convection parameterization was implemented to simulate convective clouds. Most operational climate and global numerical weather prediction models do not include aerosol-aware convection(Boucher et al., 2014), as is the case in the UM parameterization. A control simulation and enhanced aerosol simulation were run at each resolution to see how cyclones differed when aerosol was increased. In the control simulation aerosol concentration was set at a value of 100 cm^{-3} near the surface and in the enhanced aerosol simulation the accumulation mode aerosol concentration was set to 2000 cm^{-3} near the surface in the 30°N-60°N latitude band. Only liquid droplets are directly affected by the aerosol changes. For ice, number concentrations followed a simple temperature-dependent relationship, which is also not unusual of a GCM participating in the CMIP.

To understand the contributions of aerosol and meteorology to cyclones we need to characterize what constitutes a cyclone. Cyclone centers were identified by sea level pressure (SLP) (Field and Wood, 2007). Considerable research has been devoted to investigating the dependence of cyclone properties on meteorology using cyclone composites(Catto, 2016). One that has been found to be particularly useful is the so-called warm conveyor belt (WCB) metric (Field and Wood, 2007;Pfahl and Sprenger, 2016;Harrold, 1973). This relies on a simple model of cyclone development and is calculated as the product of mean wind speed and water vapor path. It should be noted that cyclone mean here and in the rest of this article refers to an average taken within 2000km of the cyclone center. WCB moisture flux is a proxy for the moisture flux ingested by the cyclone and is a good predictor of the cyclone-mean rain rate(Field and Wood, 2007). The relationship between WCB flux and rain rate appears to be relatively invariant as a function of model resolution and aerosol concentration (Fig. S1). Essentially, once in equilibrium, the water mass flux that goes into the cyclone must be precipitated out. The perturbed aerosol environment reduces the efficiency of warm rain production for a given water path and therefore should lead to a higher equilibrium water path for a given mean rain rate or WCB flux. It is interesting to note that the frozen water path in

the cyclones did not change between control and enhanced aerosol experiments, indicating that this aerosol-cyclone indirect effect acts through the warm rain process (Fig. S2).

By stratifying the cyclones simulated in the UM at GCM-surrogate and convection-permitting resolutions by the WCB moisture flux we find that WCB plays a significant role in determining the cyclone-mean precipitating and non-precipitating liquid water path (CLWP, where path is the mass in an atmospheric column) (Fig. 1a). As one might expect, a greater flux of moisture into the cyclone results in a larger total CLWP. Such a clear WCB-CLWP relationship provides a useful metric with which to stratify midlatitude cyclones. We can now ask: for a given WCB flux, do variations in the CCN available to the cyclone result in a different CLWP?

We answer this question by comparing the low and high CCN simulations and stratifying by WCB flux. This shows that for a given WCB, higher CCN translates to a higher CLWP (Fig. 1a). The difference between the control and aerosol-enhanced simulations is more pronounced in the convection-permitting model. This is because in the GCM-surrogate simulation aerosol-cloud interactions are not represented for convection, while in the convection-permitting simulation aerosol-cloud interactions are treated in the same way for all cloud elements. This indicates that the aerosol-cyclone indirect effect simulated by traditional GCMs that do not include aerosol-aware convection may be systematically too weak. Because increased CLWP results in enhanced reflection of shortwave radiation to space (Fig. S3), although thick ice clouds may mute the enhancement of reflected shortwave radiation. This implies a bias toward low climate sensitivity in traditional GCMs.

Our hypothesis, based on idealized simulations, is that *enhanced CCN should enhance CLWP in midlatitude storms for a given WCB*. In this context we now examine the observational record afforded to us by the Advanced Microwave Scanning Radiometer (AMSR(Wentz and Meissner, 2000)). The microwave radiometer is sensitive to liquid water, but it cannot distinguish rain and cloud. In the context of this paper we avoid possible ambiguity stemming from the calculation of rain rate by AMSR and refer to the sum of precipitating and non-precipitating liquid water as cyclone liquid water path (CLWP). The microwave radiometer is also able to measure water vapor path and wind speed, allowing for accurate observations of WCB moisture flux and comparison to the idealized aquaplanet simulations. Cyclone centers in the observational record are identified using SLP reanalysis from The Modern-Era Retrospective Analysis for Research and Applications version 2 (MERRA2).

Determining whether observed midlatitude cyclones have a higher or lower CCN available is more difficult than comparing high and low CCN simulations in an idealized aquaplanet. One approach would be to use the observed cloud droplet number concentration (CDNC). This provides a good proxy for CCN (Wood, 2012), but it is potentially problematic because retrieval errors relating to overlying ice cloud(Sourdeval et al., 2016), cloud heterogeneity (Grosvenor and Wood, 2014;Sourdeval et al., 2016), and low sun-angle(Grosvenor and Wood, 2014) may spuriously bias the measurements making it difficult to interpret any observed covariation between cyclone properties and CDNC. To avoid these ambiguities we take a similar approach to previous studies and use sulfate mass concentration at the surface from reanalysis as a proxy for CCN (McCoy et al., 2017;McCoy et al., 2015). The data set used to describe sulfate mass concentration is the MERRA2 reanalysis (Molod et al., 2015). This is advantageous because it is not susceptible to retrieval error and because MERRA2 does not

have a parameterized cloud-aerosol indirect effect, further simplifying its interpretation as a proxy of CCN. Using the daily mean MERRA2 SO4 we calculate a CDNC proxy within cyclones following the relationship established in previous studies (McCoy et al., 2017) (Fig. 2). The CDNC derived from reanalysis SO4 and Moderate Resolution Imaging Spectroradiometer (MODIS) CDNC over regions where the MODIS CDNC retrieval is reliable have been shown to be highly consistent with each other(McCoy et al., 2017). An enhancement in proxy CDNC occurs in the southwest quadrant that is likely to be the source of moisture and aerosol for the cyclone(Cooper et al., 2004;Naud et al., 2016;Joos et al., 2016). Because of this in this study the southwest quadrant of the cyclone composited CDNC proxy from MERRA2 will be used to stratify cyclones by CCN and will be referred to as $CDNC_{SW}$. For comparison to MERRA2-inferred CDNC the CDNC from MODIS is also composited on cyclone centers (Fig. S4) (Cooper et al., 2004;Naud et al., 2016).

Using WCB as a measure of the meteorological condition and $CDNC_{SW}$ as a measure of CCN flux into the cyclone we may evaluate the observational record and compare it to the aquaplanet simulations of aerosol enhancement. When we compare the observational record of cyclone-mean CLWP by stratifying it into the top and bottom third of observed $CDNC_{SW}$ inferred from MERRA2 (Fig. 3) a systematic separation in mean CLWP between high and low CCN cyclones becomes apparent (Fig. 1b). This separation is also clear if MODIS CDNC is used in place of MERRA2-inferred CDNC, indicating that this effect is robust to our choice of CCN proxy (Fig. 1b). Furthermore, inspection of the composite cyclone structure indicates that the increases in CLWP share features between observations and modelling, primarily an increase in CLWP in the south-west sector of the cyclone (Fig. S5).

To offer a more accurate prediction of 21st century climate change the key variable to constrain is the change in reflected shortwave radiation due to aerosol indirect effects. The cyclone-mean albedo of storms whose $CDNC_{SW}$ is in the top third of observations is higher than the albedo of cyclones in the bottom third of observed $CDNC_{SW}$ values (Fig. 4a). This is commensurate with a difference in reflected shortwave radiation between 2.2Wm^{-2} and 4.2Wm^{-2} (Fig. 4a), depending on whether MODIS CNDC or MERRA2 CDNC is used to calculate $CDNC_{SW}$ and assuming a constant downward flux consistent with the annual-mean insolation averaged between 30°-80°. Examination of the difference in albedo for cyclones in the aquaplanet simulations also demonstrates a higher albedo for enhanced CCN simulations (Fig. 4b). However, the change in reflected shortwave radiation for the GCM-surrogate simulation is only 70% of the change in reflected shortwave radiation in the convection-permitting simulation.

This analysis, while it shows that there is an aerosol indirect effect on midlatitude cyclones, does not distinguish between the changes in albedo due to changes in CDNC and changes in LWP. A better observational knowledge of cyclone ice properties would allow radiative transfer calculations that could elucidate this. However, we have shown that variation in aerosol as characterized by sulfate (McCoy et al., 2017) are consistent with observed changes in $CDNC_{SW}$ (Fig. S4c, Fig. 1b), and these variations in CDNC are consistent with variation in CLWP (Fig. 1b). Based on this evidence and the behavior of high resolution simulations (Fig. 4b) it appears that the combined effects of changes in CDNC and changes in CLWP alter cyclone-mean albedo. It should be noted that MERRA2-inferred CDNC will be used for the analysis presented below.

Atmos. Chem. Phys. Discuss., https://doi.org/10.5194/acp-2017-649
Manuscript under review for journal Atmos. Chem. Phys.
Discussion started: 4 August 2017

Atmospheric Chemistry and Physics Discussions

Given the pervasiveness of the relationships between CLWP, MERRA2-inferred $CDNC_{SW}$, and WCB we create a simple regression model of CLWP. The relationship between CLWP, WCB and $CDNC_{SW}$ shows differing behavior as a function of $CDNC_{SW}$ with a stronger increase in CLWP for a given increase in $CDNC_{SW}$ in more pristine (low $CDNC_{SW}$) storms (Fig. 5). Using the observational record from 2003-2015 we train a regression model

$$CLWP = 0.037\, WCB^{0.59} CDNC_{SW}^{0.13} - 0.0096 \quad (1)$$

where WCB is in units of mm/day, CDNC is in cm^{-3}, and CLWP is in mm. The model explains 51% of the variance in CLWP over the observational record and fits the CLWP behavior well at low $CDNC_{SW}$ (Fig. 5). This last point is important because the correct portrayal of cloud-aerosol interactions in low aerosol natural environments has a dominant effect on indirect forcing uncertainty (Carslaw et al., 2013).

We estimate the relative contributions of a standardized perturbation in meteorology and in aerosol using Eq. 1 by taking partial derivatives with respect to WCB and $CDNC_{SW}$ to give the change in CLWP for a unit change in WCB and $CDNC_{SW}$. This is scaled by the standard deviation of WCB and $CDNC_{SW}$ over the observational record to get the change in CLWP for a standard deviation change in each predictor. The ratio of the change in CLWP for a standard deviation in $CDNC_{SW}$ to the change due to a standard deviation in WCB is shown in Fig. 6.

Based on this we can see that changes in CLWP for very pristine ($CDNC_{SW}$<60cm^{-3}), large cyclones (WCB>4 mm/day) due to unit standard deviation perturbation in $CDNC_{SW}$ are estimated to be as large as 70% of those from a standard deviation perturbation in meteorology (WCB flux), while very polluted ($CDNC_{SW}$<120cm^{-3}), small cyclones (WCB<2mm/day) are nearly insensitive to changes in $CDNC_{SW}$. Averaged over the observational record, the mean relative contribution of aerosol changes is 30% based on the distribution of cyclones in $CDNC_{SW}$ and WCB space.

3.2 The 2014-2015 Holuhraun eruption in Iceland as a case study of aerosol-cyclone interactions

Our analysis of the observational record shows a relationship between CCN, as inferred by MERRA2, and CLWP for a given meteorological environment. In this section we present a case study of a transient increase in volcanic sulfate aerosol mass concentrations resulting from the 2014-2015 eruption at Holuhraun in Iceland during September and October 2014. On average, the eruption released about three times the amount of sulfur dioxide per day as all European sources combined (Schmidt et al., 2015), making it a unique case-study to evaluate enhancement of cyclone properties in the North Atlantic region(Gettelman et al., 2015). During September and October of 2014 a substantial change in cloud droplet radius was observed, but without accounting for synoptic activity no clear second indirect effect could be measured in the regional mean liquid water path (McCoy and Hartmann, 2015;Malavelle et al., 2017).

The Holuhraun case-study is particularly useful because the MERRA2 reanalysis does not include emissions from specific eruptions in its inventory after 2010(Randles et al., 2016). This means that the CDNC inferred from MERRA2 will not

capture the enhancement in $CDNC_{SW}$ due to the eruption. We exploit this by using the regression model described in the last section to calculate the CLWP consistent with AMSR-observed WCB moisture flux and MERRA2-inferred $CDNC_{SW}$. If the CLWP during the eruption is observed to be higher than the CLWP predicted by the regression model trained on the historical record, and is outside the residual error of the regression model over the course of the historical record, then that is a good indication that the sulfur emissions from the eruption altered cloud properties over the North Atlantic because MERRA2 will not include these sulfur emissions in its reanalysis.

Lagrangian simulations of the boundary layer SO4 mass concentration contingent on the Holuhraun eruption were used to evaluate whether a given cyclone center had interacted with the volcanic plume. Holuhraun sulfate was simulated originating at an altitude of 1500-3000m. The mean SO4 mass concentration from the eruption in a 2000km radius quarter circle southwest of the center of each interacting cyclone was calculated for both simulations (Fig. 7). If the Holuhraun sulfate is plotted against the difference between CLWP predicted by the regression model based on WCB and MERRA2-inferred $CDNC_{SW}$ it becomes clear that the regression model underestimates CLWP for cyclones that were substantially influenced by volcanic sulfate (mean sulfate>2ug/m3, Fig. 8). The observed anomalies in CLWP during September and October 2014 for volcanically influenced cyclones relative to the regression model's predicted CLWP are different to the anomalies present during September and October over the North Atlantic for all the other years of the observational record if a threshold of $2\mu g/m^3$ of volcanic sulfate is used to separate cyclones that have interacted with the volcanic plume from those that have not (Fig. S6). According to a two-sided rank-sum test the anomalies in CLWP where Holuhraun sulfate exceeds 2µg/m3 are different than all other Septembers and Octobers at p=0.02. This result is different than previous attempts to use Holuhraun as a constraint on the second indirect effect that could not detect a change in cloud liquid water path(Malavelle et al., 2017). One difference between previous studies and the present study is that we use 13 years of remote sensing observations to account for meteorological variability, which would otherwise obscure changes due to aerosol. Our use of convection-permitting simulations allow us to resolve a greater fraction of cloud-aerosol interaction revealing a stronger aerosol-cyclone indirect effect than in a traditional GCM that is insensitive to aerosol-cloud interactions in convective clouds. This can be seen in Fig. 1, which shows a much clearer separation between high and low aerosol simulations in the convection permitting simulation than in the GCM surrogate.

It is also important to note that this result appears to be sensitive to the diffusion and transport of the sulfate from Holuhraun. In a second simulation where the emissions height was moved to be between 0-1500m, which is lower than emissions heights during September (Schmidt et al., 2015), the cyclones identified to have interacted with the plume were not systematically different than any other year. It appears that if the Holuhraun eruption is to be used as a transient constraint on aerosol indirect effects then the volcanology surrounding the eruption will play an important role in this constraint. It is also clear that understanding the meteorology surrounding the eruption will be key in using this case as a constraint based on the difficulty in disentangling synoptic noise from cloud-aerosol interactions faced in previous studies(Malavelle et al., 2017;McCoy and Hartmann, 2015).

4. Conclusions

Based on insight gained by the investigation of high-resolution, convection-permitting idealized global simulations we have hypothesized that cyclone liquid water path is substantially influenced by aerosol perturbations providing an important key to evaluating and constraining the second indirect effect in models and offering a more tightly-constrained estimate of anthropogenic radiative forcing and of 21st century warming. The notion of an aerosol-cyclone indirect effect is supported by a case study of a transient increase in sulfate aerosol mass concentration in the North Atlantic region, resulting from the 2014-2015 eruption at Holuhraun in Iceland. Evaluation of changes in reflected shortwave radiation indicate that the aerosol-cyclone indirect effect can contribute to the total anthropogenic aerosol indirect effect.

Based on the idealized simulations and analysis of observations shown here we have developed and tested the hypothesis that cyclones with the same WCB moisture flux have a larger LWP with more aerosol. It is possible that this effect is not constrained to midlatitude cyclones and we may speculate that clouds in other regimes whose rain rate is the same have a higher LWP with increasing aerosol.

Several important conclusions can be reached based on this study. Firstly, it establishes the existence of an aerosol indirect effect on midlatitude storms. This effect has been predicted by simulations of the North Pacific (Wang et al., 2014;Joos et al., 2016), but this is the first time it has been demonstrated using observations on a global scale. Secondly, we find that the aerosol-cyclone effect is 1.4 times larger in our convection-permitting model compared to the GCM-surrogate simulation. This implies that there could be systematic biases in the aerosol indirect effect calculated by traditional GCMs, whose convective clouds are not sensitive to aerosol, and by extension we expect a spuriously low climate sensitivity in current GCMs.

Author contributions

DTM and PRF planned the paper and wrote the text. DTM performed data analysis and calculations. PRF created simulations in the Unified Model. DPG created the CDNC data set. AS performed simulations of Holuhraun's eruption. BJS, AAH, and JMW created the CASIM microphysics package. All authors contributed ideas and helped edit the paper.

Acknowledgments

AMSR data are produced by Remote Sensing Systems and were sponsored by the NASA AMSR-E Science Team and the NASA Earth Science MEaSUREs Program. Data are available at www.remss.com. MERRA2 data was downloaded from the Giovanni data server. CERES data was downloaded through the ceres.larc.nasa.gov ordering interface. DTM and PRF acknowledge support from the PRIMAVERA project, funded by the European Union's Horizon 2020 programme, Grant Agreement no. 641727.

References

Albrecht, B. A.: Aerosols, Cloud Microphysics, and Fractional Cloudiness, Science, 245, 1227-1230, 10.1126/science.245.4923.1227, 1989.

Andreae, M. O., Jones, C. D., and Cox, P. M.: Strong present-day aerosol cooling implies a hot future, Nature, 435, 1187, 2005.

Bender, F. A. M., Engstrom, A., and Karlsson, J.: Factors Controlling Cloud Albedo in Marine Subtropical Stratocumulus Regions in Climate Models and Satellite Observations, Journal of Climate, 29, 3559-3587, 10.1175/jcli-d-15-0095.1, 2016.

Bosilovich, M., Akella, S., Coy, L., Cullather, R., Draper, C., and Gelaro, R.: MERRA-2. Initial evaluation of the climate, Tech. Rep. Ser., Global Modeling and Data Assimilation, RD Koster, ed., NASA/TM-2015-104606, 2015.

Boucher, O., Randall, D. A., Artaxo, P., Bretherton, C., Feingold, G., Forster, P. M., Kerminen, V.-M., Kondo, Y., Liao, H., Lohmann, U., Rasch, P., Satheesh, S. K., Sherwood, S. C., Stevens, B., and Zhang, X. Y.: Clouds and Aerosols
Climate Change 2013 - The Physical Science Basis, Cambridge University Press, 2014.

Carslaw, K. S., Lee, L. A., Reddington, C. L., Pringle, K. J., Rap, A., Forster, P. M., Mann, G. W., Spracklen, D. V., Woodhouse, M. T., Regayre, L. A., and Pierce, J. R.: Large contribution of natural aerosols to uncertainty in indirect forcing, Nature, 503, 67-71, 10.1038/nature12674, 2013.

Catto, J. L.: Extratropical cyclone classification and its use in climate studies, Reviews of Geophysics, 54, 486-520, 10.1002/2016RG000519, 2016.

Charlson, R. J., Schwartz, S. E., Hales, J. M., Cess, R. D., Coakley, J. A., Hansen, J. E., and Hofmann, D. J.: Climate Forcing by Anthropogenic Aerosols, Science, 255, 423-430, 10.1126/science.255.5043.423, 1992.

Cooper, O. R., Forster, C., Parrish, D., Trainer, M., Dunlea, E., Ryerson, T., Hübler, G., Fehsenfeld, F., Nicks, D., Holloway, J., de Gouw, J., Warneke, C., Roberts, J. M., Flocke, F., and Moody, J.: A case study of transpacific warm conveyor belt transport: Influence of merging airstreams on trace gas import to North America, Journal of Geophysical Research: Atmospheres, 109, n/a-n/a, 10.1029/2003JD003624, 2004.

Cooper, W. A.: Ice initiation in natural clouds, in: Precipitation Enhancement—A Scientific Challenge, Springer, 29-32, 1986.

Ebmeier, S. K., Sayer, A. M., Grainger, R. G., Mather, T. A., and Carboni, E.: Systematic satellite observations of the impact of aerosols from passive volcanic degassing on local cloud properties, Atmos. Chem. Phys., 14, 10601-10618, 10.5194/acp-14-10601-2014, 2014.

Field, P. R., and Wood, R.: Precipitation and Cloud Structure in Midlatitude Cyclones, Journal of Climate, 20, 233-254, doi:10.1175/JCLI3998.1, 2007.

Forster, P. M.: Inference of climate sensitivity from analysis of Earth's energy budget, Annual Review of Earth and Planetary Sciences, 44, 85-106, 2016.

Gassó, S.: Satellite observations of the impact of weak volcanic activity on marine clouds, Journal of Geophysical Research: Atmospheres, 113, n/a-n/a, 10.1029/2007JD009106, 2008.

Gettelman, A., Schmidt, A., and Egill Kristjansson, J.: Icelandic volcanic emissions and climate, Nature Geosci, 8, 243-243, 10.1038/ngeo2376
http://www.nature.com/ngeo/journal/v8/n4/abs/ngeo2376.html - supplementary-information, 2015.

Grandey, B. S., Stier, P., Grainger, R. G., and Wagner, T. M.: The contribution of the strength and structure of extratropical cyclones to observed cloud–aerosol relationships, Atmos. Chem. Phys., 13, 10689-10701, 10.5194/acp-13-10689-2013, 2013.

Grosvenor, D. P., and Wood, R.: The effect of solar zenith angle on MODIS cloud optical and microphysical retrievals within marine liquid water clouds, Atmos. Chem. Phys., 14, 7291-7321, 10.5194/acp-14-7291-2014, 2014.

Grosvenor, D. P., Field, P. R., Hill, A. A., and Shipway, B. J.: The relative importance of macrophysical and cloud albedo changes for aerosol-induced radiative effects in closed-cell stratocumulus: insight from the modelling of a case study, Atmos. Chem. Phys., 17, 5155-5183, 10.5194/acp-17-5155-2017, 2017.

Gryspeerdt, E., Quaas, J., and Bellouin, N.: Constraining the aerosol influence on cloud fraction, Journal of Geophysical Research: Atmospheres, n/a-n/a, 10.1002/2015JD023744, 2016.

Harrold, T. W.: Mechanisms influencing the distribution of precipitation within baroclinic disturbances, Quarterly Journal of the Royal Meteorological Society, 99, 232-251, 10.1002/qj.49709942003, 1973.

Hartmann, D. L.: Global physical climatology, Newnes, 2015.

Hill, A. A., Shipway, B. J., and Boutle, I. A.: How sensitive are aerosol-precipitation interactions to the warm rain representation?, Journal of Advances in Modeling Earth Systems, 7, 987-1004, 10.1002/2014MS000422, 2015.

Igel, A. L., van den Heever, S. C., Naud, C. M., Saleeby, S. M., and Posselt, D. J.: Sensitivity of Warm-Frontal Processes to Cloud-Nucleating Aerosol Concentrations, Journal of the Atmospheric Sciences, 70, 1768-1783, 10.1175/JAS-D-12-0170.1, 2013.

Jones, A., Thomson, D., Hort, M., and Devenish, B.: The U.K. Met Office's Next-Generation Atmospheric Dispersion Model, NAME III, in: Air Pollution Modeling and Its Application XVII, edited by: Borrego, C., and Norman, A.-L., Springer US, Boston, MA, 580-589, 2007.

Joos, H., Madonna, E., Witlox, K., Ferrachat, S., Wernli, H., and Lohmann, U.: Effect of anthropogenic aerosol emissions on precipitation in warm conveyor belts in the western North Pacific in winter – a model study with ECHAM6-HAM, Atmos. Chem. Phys. Discuss., 2016, 1-20, 10.5194/acp-2016-722, 2016.

King, M. D., Menzel, W. P., Kaufman, Y. J., Tanre, D., Bo-Cai, G., Platnick, S., Ackerman, S. A., Remer, L. A., Pincus, R., and Hubanks, P. A.: Cloud and aerosol properties, precipitable water, and profiles of temperature and water vapor from MODIS, Geoscience and Remote Sensing, IEEE Transactions on, 41, 442-458, 10.1109/TGRS.2002.808226, 2003.

Loeb, N. G., Wielicki, B. A., Doelling, D. R., Smith, G. L., Keyes, D. F., Kato, S., Manalo-Smith, N., and Wong, T.: Toward Optimal Closure of the Earth's Top-of-Atmosphere Radiation Budget, Journal of Climate, 22, 748-766, 10.1175/2008jcli2637.1, 2009.

Lu, Y., and Deng, Y.: Impact of Environmental Aerosols on a Developing Extratropical Cyclone in the Superparameterized Community Atmosphere Model, Journal of Climate, 29, 5533-5546, 10.1175/JCLI-D-16-0157.1, 2016.

Mace, G. G., and Abernathy, A. C.: Observational evidence for aerosol invigoration in shallow cumulus downstream of Mount Kilauea, Geophysical Research Letters, 43, 2981-2988, 10.1002/2016GL067830, 2016.

Malavelle, F. F., Haywood, J. M., Jones, A., Gettelman, A., Clarisse, L., Bauduin, S., Allan, R. P., Karset, I. H. H., Kristjánsson, J. E., Oreopoulos, L., Cho, N., Lee, D., Bellouin, N., Boucher, O., Grosvenor, D. P., Carslaw, K. S., Dhomse, S., Mann, G. W., Schmidt, A., Coe, H., Hartley, M. E., Dalvi, M., Hill, A. A., Johnson, B. T., Johnson, C. E., Knight, J. R., O'Connor, F. M., Partridge, D. G., Stier, P., Myhre, G., Platnick, S., Stephens, G. L., Takahashi, H., and Thordarson, T.: Strong constraints on aerosol–cloud interactions from volcanic eruptions, Nature, 546, 485-491, 10.1038/nature22974 http://www.nature.com/nature/journal/v546/n7659/abs/nature22974.html - supplementary-information, 2017.

Marshall, J., and Palmer, W.: THE DISTRIBUTION OF RAINDROPS WITH SIZE, Journal of Meteorology, 5, 165-166, 10.1175/1520-0469(1948)005<0165:tdorws>2.0.co;2, 1948.

McCoy, D. T., Burrows, S. M., Wood, R., Grosvenor, D. P., Elliott, S. M., Ma, P.-L., Rasch, P. J., and Hartmann, D. L.: Natural aerosols explain seasonal and spatial patterns of Southern Ocean cloud albedo, Science Advances, 1, 2015.

McCoy, D. T., and Hartmann, D. L.: Observations of a substantial cloud-aerosol indirect effect during the 2014–2015 Bárðarbunga-Veiðivötn fissure eruption in Iceland, Geophys. Res. Lett., n/a-n/a, 10.1002/2015GL067070, 2015.

McCoy, D. T., Bender, F. A. M., Mohrmann, J. K., Hartmann, D. L., Wood, R., and Grosvenor, D. P.: The global aerosol-cloud first indirect effect estimated using MODIS, MERRA and AeroCom, Journal of Geophysical Research: Atmospheres, n/a-n/a, 10.1002/2016JD026141, 2017.

Meskhidze, N., and Nenes, A.: Phytoplankton and Cloudiness in the Southern Ocean, Science, 314, 1419-1423, 10.1126/science.1131779, 2006.

Molod, A., Takacs, L., Suarez, M., and Bacmeister, J.: Development of the GEOS-5 atmospheric general circulation model: evolution from MERRA to MERRA2, Geosci. Model Dev., 8, 1339-1356, 10.5194/gmd-8-1339-2015, 2015.

Nakajima, T., Higurashi, A., Kawamoto, K., and Penner, J. E.: A possible correlation between satellite-derived cloud and aerosol microphysical parameters, Geophys. Res. Lett., 28, 1171-1174, 10.1029/2000GL012186, 2001.

Naud, C. M., Posselt, D. J., and van den Heever, S. C.: Aerosol optical depth distribution in extratropical cyclones over the Northern Hemisphere oceans, Geophysical Research Letters, 43, 10,504-510,511, 10.1002/2016GL070953, 2016.

Pfahl, S., and Sprenger, M.: On the relationship between extratropical cyclone precipitation and intensity, Geophysical Research Letters, 43, 1752-1758, 10.1002/2016GL068018, 2016.

Quaas, J., Boucher, O., Bellouin, N., and Kinne, S.: Satellite-based estimate of the direct and indirect aerosol climate forcing, Journal of Geophysical Research: Atmospheres, 113, n/a-n/a, 10.1029/2007JD008962, 2008.

Randles, C., AM, d. S., V, B., A, D., PR, C., V, A., H, B., EP, N., X, P., A, S., H, Y., and R, G.: The MERRA-2 Aerosol Assimilation, Technical Report Series on Global Modeling and Data Assimilation, 45, 2016.

Rogers, R., and Yau, M.: A short course of cloud physics. Pregamon, in, Oxford, 1989.

Schmidt, A., Carslaw, K. S., Mann, G. W., Rap, A., Pringle, K. J., Spracklen, D. V., Wilson, M., and Forster, P. M.: Importance of tropospheric volcanic aerosol for indirect radiative forcing of climate, Atmos. Chem. Phys., 12, 7321-7339, 10.5194/acp-12-7321-2012, 2012.

Schmidt, A., Leadbetter, S., Theys, N., Carboni, E., Witham, C. S., Stevenson, J. A., Birch, C. E., Thordarson, T., Turnock, S., Barsotti, S., Delaney, L., Feng, W., Grainger, R. G., Hort, M. C., Höskuldsson, Á., Ialongo, I., Ilyinskaya, E., Jóhannsson, T., Kenny, P., Mather, T. A., Richards, N. A. D., and Shepherd, J.: Satellite detection, long-range transport, and air quality impacts of volcanic sulfur dioxide from the 2014–2015 flood lava eruption at Bárðarbunga (Iceland), Journal of Geophysical Research: Atmospheres, n/a-n/a, 10.1002/2015JD023638, 2015.

Sekiguchi, M., Nakajima, T., Suzuki, K., Kawamoto, K., Higurashi, A., Rosenfeld, D., Sano, I., and Mukai, S.: A study of the direct and indirect effects of aerosols using global satellite data sets of aerosol and cloud parameters, Journal of Geophysical Research: Atmospheres, 108, n/a-n/a, 10.1029/2002JD003359, 2003.

Shipway, B. J., and Hill, A. A.: Diagnosis of systematic differences between multiple parametrizations of warm rain microphysics using a kinematic framework, Quarterly Journal of the Royal Meteorological Society, 138, 2196-2211, 10.1002/qj.1913, 2012.

Sourdeval, O., Labonnote, L. C., Baran, A. J., Mülmenstädt, J., and Brogniez, G.: A Methodology for Simultaneous Retrieval of Ice and Liquid Water Cloud Properties. Part II: Near-global Retrievals and Evaluation against A-Train Products, Quarterly Journal of the Royal Meteorological Society, 2016.

Stevens, B., and Feingold, G.: Untangling aerosol effects on clouds and precipitation in a buffered system, Nature, 461, 607-613, 2009.

Thompson, G., and Eidhammer, T.: A Study of Aerosol Impacts on Clouds and Precipitation Development in a Large Winter Cyclone, Journal of the Atmospheric Sciences, 71, 3636-3658, 10.1175/JAS-D-13-0305.1, 2014.

Twomey, S.: INFLUENCE OF POLLUTION ON SHORTWAVE ALBEDO OF CLOUDS, Journal of the Atmospheric Sciences, 34, 1149-1152, 10.1175/1520-0469(1977)034<1149:tiopot>2.0.co;2, 1977.

Walters, D., Boutle, I., Brooks, M., Melvin, T., Stratton, R., Vosper, S., Wells, H., Williams, K., Wood, N., Allen, T., Bushell, A., Copsey, D., Earnshaw, P., Edwards, J., Gross, M., Hardiman, S., Harris, C., Heming, J., Klingaman, N., Levine, R., Manners, J., Martin, G., Milton, S., Mittermaier, M., Morcrette, C., Riddick, T., Roberts, M., Sanchez, C., Selwood, P., Stirling, A., Smith, C., Suri, D., Tennant, W., Vidale, P. L., Wilkinson, J., Willett, M., Woolnough, S., and Xavier, P.: The Met Office Unified Model Global Atmosphere 6.0/6.1 and JULES Global Land 6.0/6.1 configurations, Geosci. Model Dev., 10, 1487-1520, 10.5194/gmd-10-1487-2017, 2017.

Wang, Y., Wang, M., Zhang, R., Ghan, S. J., Lin, Y., Hu, J., Pan, B., Levy, M., Jiang, J. H., and Molina, M. J.: Assessing the effects of anthropogenic aerosols on Pacific storm track using a multiscale global climate model, Proceedings of the National Academy of Sciences, 111, 6894-6899, 10.1073/pnas.1403364111, 2014.

Wentz, F., and Meissner, T.: AMSR Ocean Algorithm, Version 2, Remote Sensing Systems, Santa Rosa, CA., report number 121599A-1, 66 pp., 2000.

Wielicki, B. A., Barkstrom, B. R., Harrison, E. F., III, R. B. L., Smith, G. L., and Cooper, J. E.: Clouds and the Earth's Radiant Energy System (CERES): An Earth Observing System Experiment, Bulletin of the American Meteorological Society, 77, 853-868, 10.1175/1520-0477(1996)077<0853:catere>2.0.co;2, 1996.

Wood, R.: Stratocumulus Clouds, Monthly Weather Review, 140, 2373-2423, 10.1175/MWR-D-11-00121.1, 2012.

Yuan, T., Remer, L. A., and Yu, H.: Microphysical, macrophysical and radiative signatures of volcanic aerosols in trade wind cumulus observed by the A-Train, Atmos. Chem. Phys., 11, 7119-7132, 10.5194/acp-11-7119-2011, 2011.

Atmos. Chem. Phys. Discuss., https://doi.org/10.5194/acp-2017-649
Manuscript under review for journal Atmos. Chem. Phys.
Discussion started: 4 August 2017

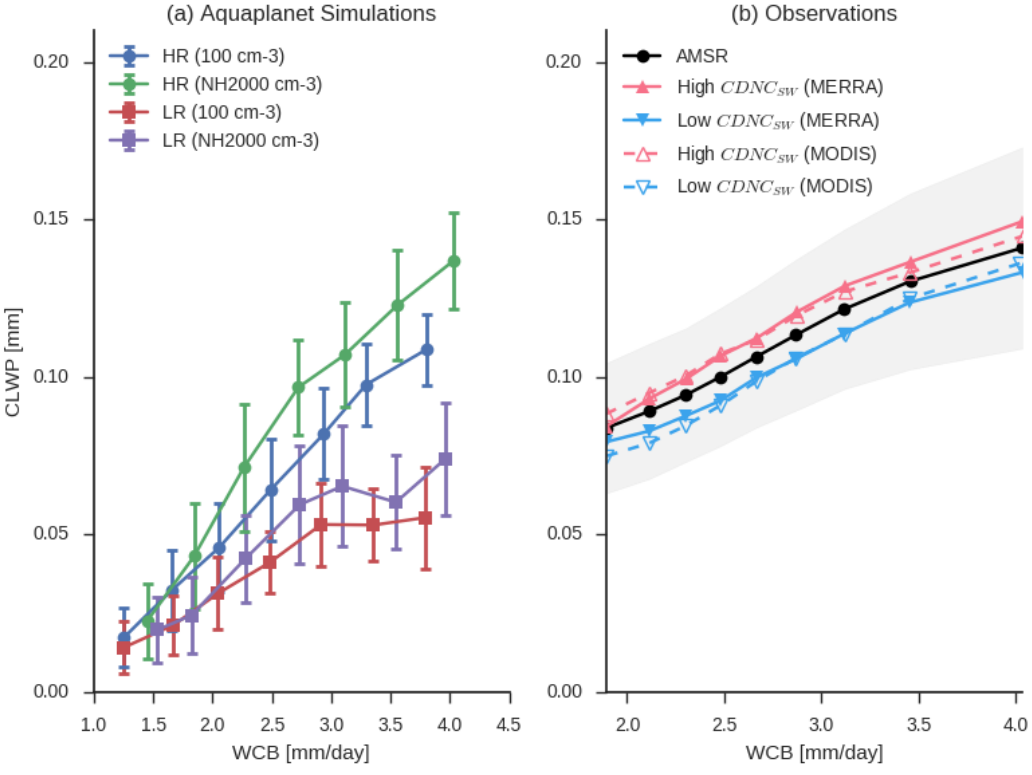

Fig. 1 Comparison between the dependence of cyclone mean liquid water path (CLWP) on warm conveyor belt (WCB) moisture flux as a function of increasing aerosol in (a) a suite of global aquaplanet simulations and (b) in observations between 2003 and 2015. Aquaplanet simulations are run at convection-permitting (HR) and GCM-surrogate resolution (LR). In (a) the CLWP is binned by WCB and standard deviations in CLWP across bins are shown as error bars. In the aquaplanet simulations a high aerosol channel is added to the northern hemisphere to investigate the response of cyclone properties and surface accumulation mode aerosol concentrations are noted in the legend. In (b) the CLWP observed by AMSR is binned by WCB. Standard deviation across each bin is shown as a shaded grey area. Cyclones with MERRA2-inferred $CDNC_{SW}$ (Fig. 2) in the top and bottom third of observed $CDNC_{SW}$ (see Fig. 3) are indicated by red and blue lines. Dashed lines show the CLWP if MODIS observed $CDNC_{SW}$ is used in place of MERRA2-inferred $CDNC_{SW}$.

Atmos. Chem. Phys. Discuss., https://doi.org/10.5194/acp-2017-649
Manuscript under review for journal Atmos. Chem. Phys.
Discussion started: 4 August 2017

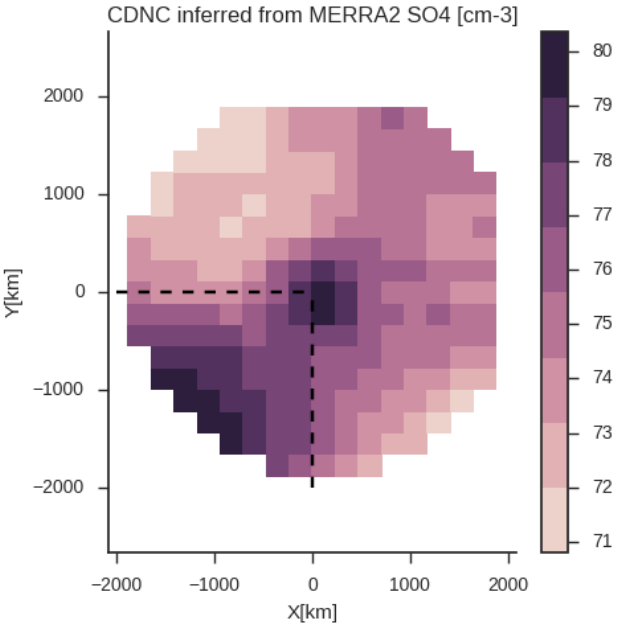

Fig. 2 Cloud droplet number concentration (CDNC) inferred from planetary boundary layer sulfate aerosol mass concentrations in units of cm^{-3} simulated in the MERRA2 reanalysis (McCoy et al., 2017) composited around cyclone centers from 2003-2015. The CDNC in the southwest quadrant ($CDNC_{SW}$ is highlighted with dashed lines) is used as a proxy for CCN being imported into the cyclone.

Atmos. Chem. Phys. Discuss., https://doi.org/10.5194/acp-2017-649
Manuscript under review for journal Atmos. Chem. Phys.
Discussion started: 4 August 2017

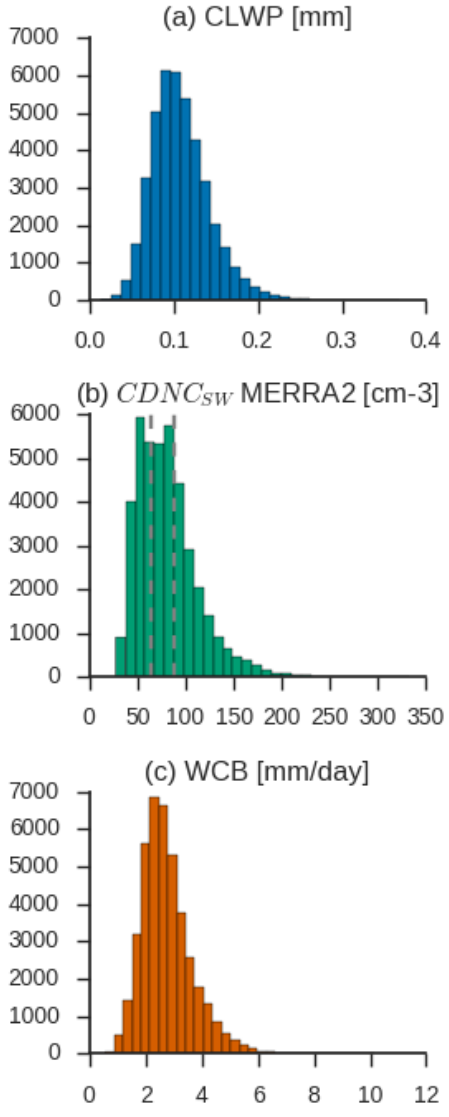

Fig. 3 Distributions of cyclone-mean properties within the 2003-2015 observational record. Units are noted for each variable. The number of composite cyclones with that value is indicated on the ordinate. In (b) the top and bottom third of distribution are indicated with dashed lines.

Atmos. Chem. Phys. Discuss., https://doi.org/10.5194/acp-2017-649
Manuscript under review for journal Atmos. Chem. Phys.
Discussion started: 4 August 2017

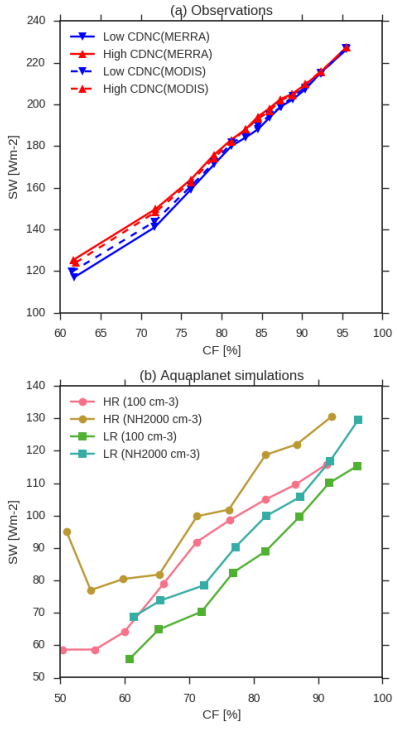

Fig. 4 (a) The difference in reflected shortwave (SW) at the top of atmosphere (TOA) between the top and bottom third of all observed $CDNC_{SW}$ (see Fig. 1b). Both MERRA2 sulfate and MODIS-observed $CDNC_{SW}$ are used to partition the top and bottom third of $CDNC_{SW}$ and are noted in the legend. The reflected SW is calculated using the CERES SYN1DEG albedo. The albedo is scaled by the annual mean insolation between 30°-80° to calculate the reflected SW. Albedo scaled by annual mean insolation is plotted as a function of cloud fraction, which determines most of its variance (Bender et al., 2016). Reflected SW is binned in equal quantiles of cloud fraction. (b) shows cyclone-mean SW from the aquaplanet simulations for high and low CCN and convection-permitting (HR) and GCM-surrogate simulations (LR).

Atmos. Chem. Phys. Discuss., https://doi.org/10.5194/acp-2017-649
Manuscript under review for journal Atmos. Chem. Phys.
Discussion started: 4 August 2017

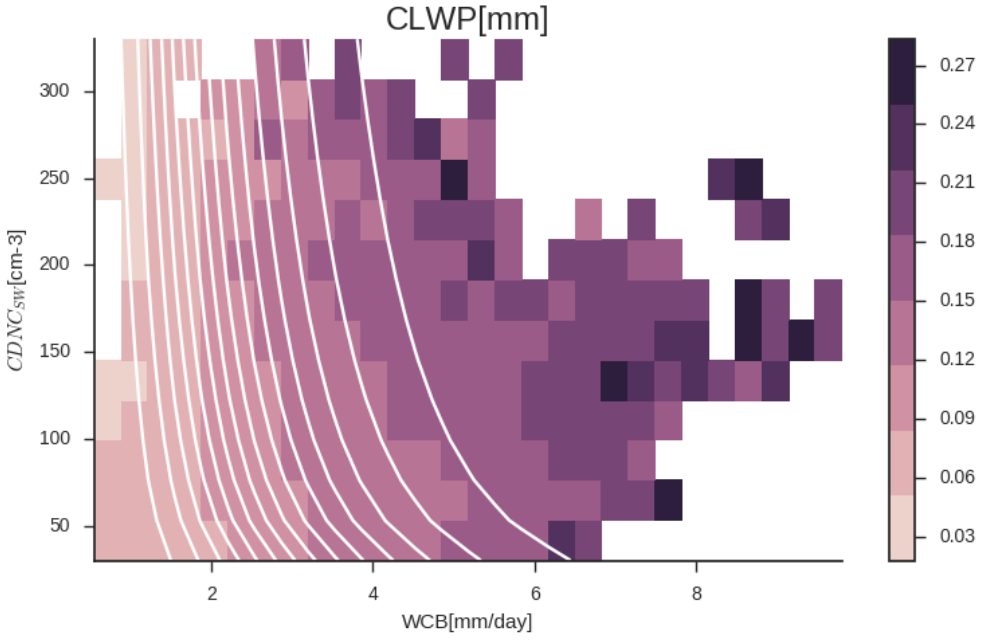

Fig. 5 The cyclone-mean CLWP in units of mm of liquid water observed by AMSR binned as a function of WCB moisture flux and MERRA2-inferred $CDNC_{SW}$ (see Fig. 2). White lines show contours of constant CLWP as predicted by Eq. 1 while colors show binned observations of CLWP.

Atmos. Chem. Phys. Discuss., https://doi.org/10.5194/acp-2017-649
Manuscript under review for journal Atmos. Chem. Phys.
Discussion started: 4 August 2017

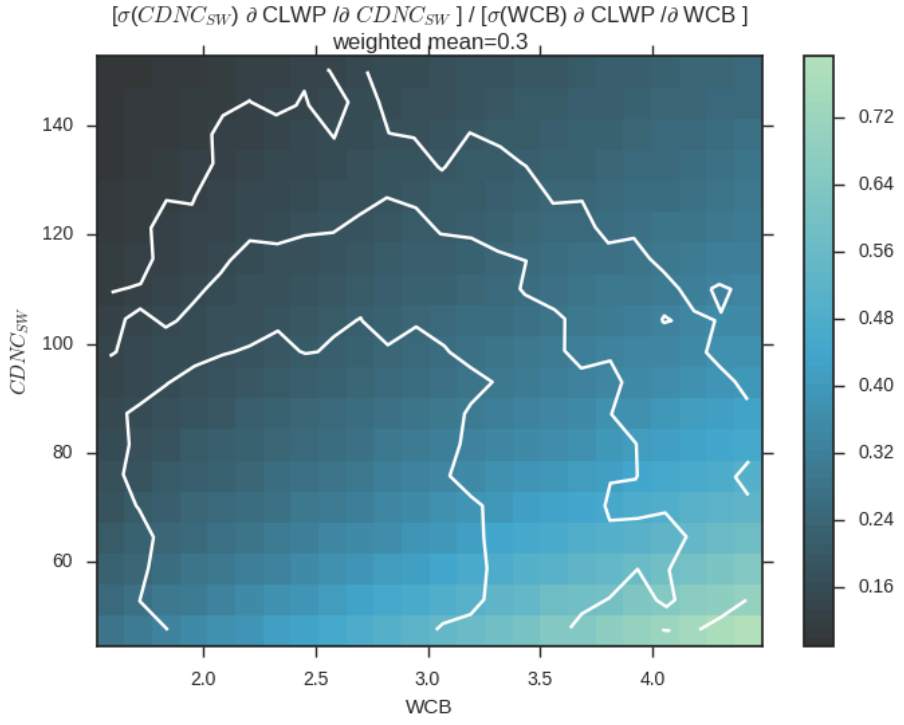

Fig. 6 The relative contribution to CLWP of perturbations in $CDNC_{SW}$ and perturbations in WCB as estimated using Eq. 1 and the standard deviation of each predictor over the historical record. The partial derivative of Eq. 1 is taken with respect to each predictor and scaled by the standard deviation of that predictor. The ratio of the partial derivative scaled by standard deviations in each of the predictors is shown using colors. The 25, 50, and 75th percentile of the joint probability distribution of cyclones during the observational record are shown as white lines. The joint probability distribution is used to calculate the weighted mean of the fractional contribution of perturbations in $CDNC_{SW}$ and WCB over the range of WCB and $CDNC_{SW}$ in the observational record.

Atmos. Chem. Phys. Discuss., https://doi.org/10.5194/acp-2017-649
Manuscript under review for journal Atmos. Chem. Phys.
Discussion started: 4 August 2017

Atmospheric Chemistry and Physics Discussions

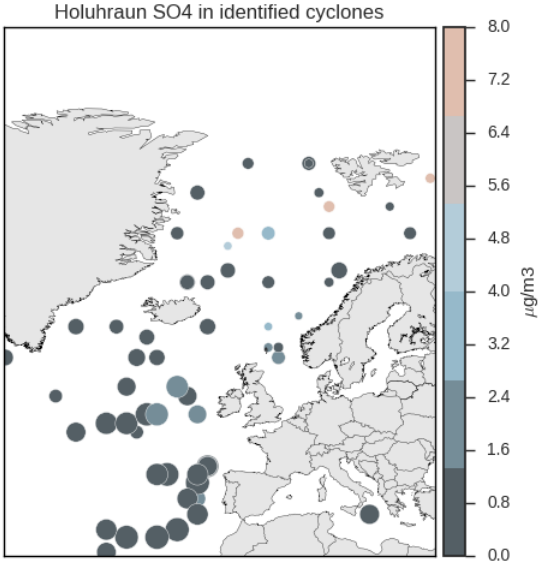

Fig. 7 Cyclone centers during September and October of 2014. The size of each dot indicates the WCB moisture flux observed for that cyclone. The color refers to the dispersion model-simulated sulfate mass concentration from Holuhraun.

Atmos. Chem. Phys. Discuss., https://doi.org/10.5194/acp-2017-649
Manuscript under review for journal Atmos. Chem. Phys.
Discussion started: 4 August 2017

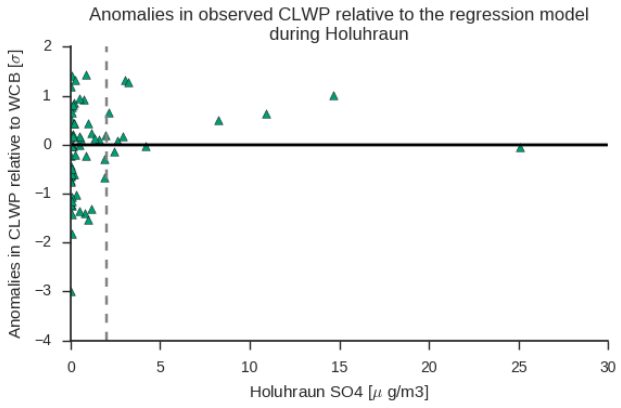

Fig. 8 Cyclone-mean CLWPs in the North Atlantic (50°W-30°E) during the Holuhraun eruption of September and October of 2014 were found to be higher than expected by the regression model (Eq. 1) prediction based on observed meteorology and the background sulfate mass concentrations modeled by MERRA2 without emissions from Holuhraun. The boundary layer (100-900 m) sulfate from the eruption calculated by the NAME dispersion model in the southwest quadrant of each cyclone is shown on the x-axis. A sulfate concentration of 2 μg/m^3 originating from Holuhraun is taken to indicate cyclones that were substantially influenced by Holuhraun and is shown as a dashed line (see Fig. S6). The y-axis shows the anomalies in CLWP observed by AMSR relative to the CLWP predicted by with AMSR-observed WCB and MERRA2-inferred $CDNC_{SW}$. Anomalies in CLWP are expressed in standard deviations at a given WCB (see grey shading in Fig. 1b).